

# CHEMISTRY

## A European Journal

A Journal of



[www.chemeurj.org](http://www.chemeurj.org)



## Reprint



WILEY-VCH

## ■ Chromophores | Hot Paper |

## Solvent-Sensitive Emitting Urea-Bridged bis-BODIPYs: Ready Access by a One-Pot Tandem Staudinger/Aza-Wittig Ureation

J. Cristóbal López,\*<sup>[a]</sup> Mayca del Rio,<sup>[a]</sup> Ainhoa Oliden,<sup>[b]</sup> Jorge Bañuelos,\*<sup>[b]</sup> Iñigo López-Arbeloa,<sup>[b]</sup> Inmaculada García-Moreno,<sup>[c]</sup> and Ana M. Gómez\*<sup>[a]</sup>

Dedicated to Prof. Antonio Lorente (UAH) on the occasion of his retirement.

**Abstract:** Herein we describe the synthesis, and computationally aided photophysical characterization of a new set of urea-bridged bis-BODIPY derivatives. These new dyads are efficiently obtained by a one-pot tandem Staudinger/aza-Wittig ureation protocol, from easily accessible *meso*-phenyl *ortho*-azidomethyl BODIPYs. These symmetric bis-BODIPYs outstand by a high absorption probability and excellent fluorescence and laser emission in less polar media. Never-

theless, this emission ability decreases in more polar media, which is ascribed to a light-induced charge-transfer from the urea spacer to the dipyrin core, a process that can be modulated by appropriate changes in the substitution pattern of the BODIPY core. Furthermore, this ureation protocol can also be employed for the direct conjugation of our BODIPY-azides to amine-containing compounds, thus providing access to fluorescent non-symmetric ureas.

## Introduction

Boron dipyrromethane (BODIPY, 4,4-difluoro-4-bora-3a,4a-diaza-s-indacene),<sup>[1]</sup> that is, **1** (Figure 1), constitute a family of widely studied chromophores and fluorophores owing to their strong UV/Vis absorption profiles and high fluorescence quantum yields ( $\phi$ ).<sup>[2]</sup> Their relevance also stems from their reasonable stability under physiological conditions, their relative insensitivity to solvent polarity, and the potential to fine-tune their spectroscopic and photophysical properties by well-documented synthetic postmodifications on the BODIPY core.<sup>[3,4]</sup> For these reasons, they have found ample application as photo-

sensitizers,<sup>[5]</sup> fluorescent labels,<sup>[6]</sup> laser-dyes,<sup>[7]</sup> and artificial light-harvesting arrays,<sup>[8]</sup> among others.<sup>[9]</sup>

More recently, the interest on covalently-linked BODIPY dimers (also termed BODIPY dyemers,<sup>[10]</sup> or bis-BODIPYs<sup>[11]</sup>) has surfaced as an additional area of interest in the field. In these derivatives, the photophysical signatures can be drastically

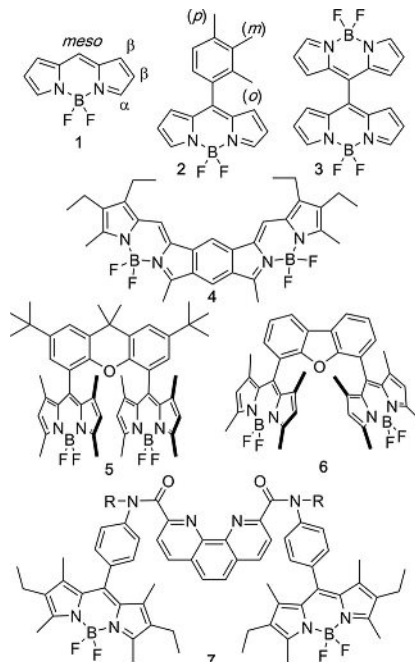


**Figure 1.** BODIPY (**1**), *meso*-aryl BODIPY (**2**); *meso*–*meso* directly linked dimer (**3**);  $\beta$ – $\beta$ -benzene  $\pi$ -fused bis-BODIPY (**4**); *meso*-*meso* tethered bis-BODIPYs (**5**, **6**); and amide-linked bichromophoric BODIPYs (**7**).

[a] Dr. J. Cristóbal López, Dr. M. del Rio, Dr. A. M. Gómez  
Bio-organic Chemistry Department  
Instituto de Química Orgánica General (IQOG-CSIC)  
Juan de la Cierva 3  
28006 Madrid (Spain)  
E-mail: jc.lopez@csic.es  
ana.gomez@csic.es

[b] A. Oliden, Dr. J. Bañuelos, Prof. I. López-Arbeloa  
Departamento Química Física  
Universidad del País Vasco-EHU  
Aptd. 644  
48080 Bilbao (Spain)  
E-mail: jorge.banuelos@ehu.es

[c] Prof. I. García-Moreno  
Departamento de Sistemas de Baja Dimensionalidad  
Superficies y Materia Condensada  
Instituto de Química Física Rocasolano  
CSIC  
Serrano 119  
28006 Madrid (Spain)

Supporting information and the ORCID identification number(s) for the author(s) of this article can be found under <https://doi.org/10.1002/chem.201703383>.

altered by changes on the position of attachment, geometrical arrangement of the units, and spacers structure, thereby spanning a wide assortment of photonic and biophotonic applications.

From a structural perspective, contributions from different research groups have focused in the generation and study of at least three kinds of dimeric structures. Directly linked BODIPYs comprising;  $\alpha$ - $\alpha$  linked,<sup>[12]</sup>  $\beta$ - $\beta$  linked,<sup>[13]</sup> *meso*- $\beta$  linked,<sup>[14]</sup> and *meso*-*meso* linked, for example, **3** (Figure 1),<sup>[14a, 15]</sup> have been studied and shown to display interesting properties. Those include the generation of electroluminescence,<sup>[12d, 16]</sup> the formation of fluorescent aggregates,<sup>[17]</sup> and their potential as singlet oxygen photosensitizers in photodynamic therapy.<sup>[14a, 18]</sup> On the other hand, the interest in highly  $\pi$ -conjugated systems, owing to their various applications as red-edge emitters, was at the origin of the attention paid to a second class of BODIPY dimers,<sup>[19]</sup> fully fused conformation-restricted BODIPY dimers, for example, **4** (Figure 1).<sup>[20]</sup> Finally, access to bridged bis-BODIPYs,<sup>[21]</sup> has given rise to a broad variety of relevant derivatives that differ in the nature of the connector or linker, and the site of tethering at the BODIPY core. In this context, although a few examples of  $\alpha$ -bridged,<sup>[3a, 10, 22]</sup>  $\beta$ -bridged,<sup>[3a, 10, 23]</sup> and even boron-bridged bis-BODIPYs,<sup>[24]</sup> have been reported most of the described derivatives are connected by linkers at the *meso*-position, either directly<sup>[25]</sup> or through a *meso*-phenyl substituent (then, *o*-, *m*-,<sup>[26]</sup> and *p*-,<sup>[27]</sup> orientations became possible, as in **2**, Figure 1).

In bridged bis-BODIPYs, the nature of the linker, flexible or rigid, short or long, influences the relative disposition of the BODIPY units. For instance, in the case of compound **5** (Figure 1),<sup>[25]</sup> a rigid dimethylxanthene spacer forces both BODIPYs to adopt a cofacial arrangement allowing an efficient energy transfer.<sup>[28]</sup> Thus, subtle variations in the nature of the rigid connector can force different relative orientations between the BODIPYs. In the case of bis-BODIPY **6** (Figure 1), a di-benzofuran spacer induced a different bite angle between the two BODIPY units, affecting their fluorescent properties.<sup>[28b]</sup> Bis-BODIPY derivatives **7** (Figure 1), recently described by Harriman and co-workers, represent an interesting example of *meso*-phenyl substituted-BODIPYs connected by amide linkages to a rigid phenanthroline core.<sup>[29]</sup> In these derivatives, it was found that an increase in solvent polarity tended to reduce their fluorescence, and this behavior was ascribed to light-induced charge-transfer between the two BODIPYs, probably facilitated by conformational changes in strongly polar media.<sup>[29]</sup> This tendency, however, was disrupted in hydrogen-bond-accepting solvents.

As part of a research project, we became interested in rotationally restricted *o*-azidomethyl *meso*-phenyl BODIPYs (**8b**) and their potential use in conjugation to biomolecules.<sup>[30]</sup> Access to BODIPYs **8b**, was initially carried out by an efficient Liebeskind-Srägl cross-coupling reaction,<sup>[31]</sup> as described by Peña-Cabrera's group.<sup>[32]</sup> More recently, we have reported access to BODIPYs **8b**, by a more expeditious method that involved a one-pot reaction of phthalide with pyrroles leading to *meso*-(*o*-hydroxymethyl) BODIPYs **8a**,<sup>[33]</sup> followed by a synthetic  $\text{CH}_2\text{OH} \rightarrow \text{CH}_2\text{N}_3$ , transformation.<sup>[34]</sup>

In this manuscript, we describe the synthesis and computationally aided photophysical properties of urea-bridged bis-BODIPYs **9**, which are available by a one-step reaction of BODIPY azides, **8b**, *vide infra* (Figure 2). Furthermore, the method has also been applied to the synthesis of non-symmetric ureas, thus making possible the BODIPY conjugation to amino derivatives.

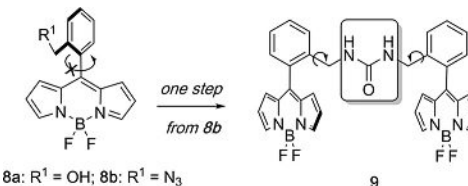


Figure 2. Urea-bridged bis-BODIPYs (**9**), available from *o*-azidomethyl *meso*-phenyl BODIPYs (**8b**) by a one-step process.

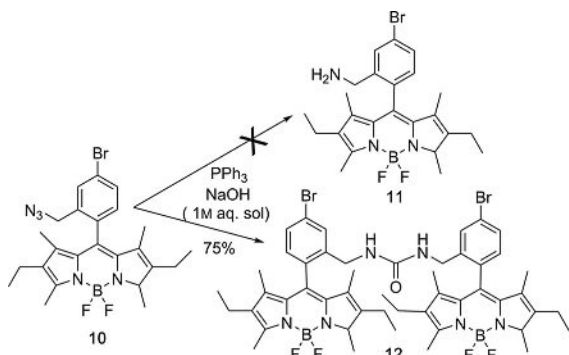
In our opinion, urea-bridged bis-BODIPYs, for example **9**, could be of relevance for several reasons: i) the planarity of the urea linkage leads to a well-defined organization of its substituents,<sup>[35]</sup> which in conjunction with the restricted rotation about the *meso*-(*o*-phenyl) bond in each BODIPY unit,<sup>[36]</sup> might lead to geometrically organized systems, ii) ureas are good hydrogen donors, since their two parallel NH bonds are perfectly suited for coordination, iii) ureas have also found utility as organocatalysts and anion transporters, among others, and iv) even though, only scarce examples of BODIPY containing ureas have been reported,<sup>[37]</sup> they have been shown to display interesting coordinating properties towards phosphate, pyrophosphate and fluoride anions.<sup>[38, 39]</sup>

## Results and Discussion

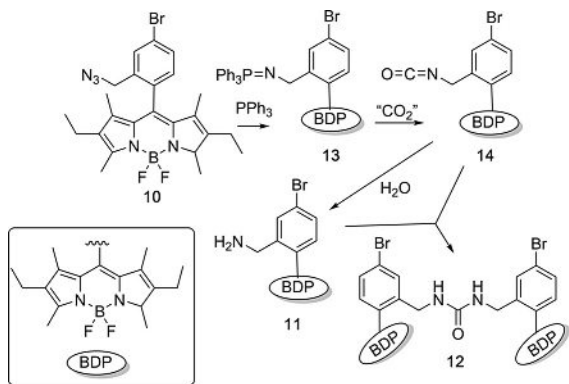
### Synthesis

As previously mentioned, our interest in the preparation of conjugatable BODIPYs had led us to the preparation of several BODIPY derivatives (including formyl and isothiocyanyl derivatives).<sup>[34]</sup> In this context, to gain access to BODIPY-amines, we attempted the well-known Staudinger "azido  $\rightarrow$  amino" transformation (PPh<sub>3</sub>, aq. NaOH),<sup>[40]</sup> from BODIPY-azide, **10** (Scheme 1). However, Staudinger reduction of **10** did not lead to the desired BODIPY amine **11**, and instead, bridged-urea bis-BODIPY **12** could be isolated in fairly good yields (Scheme 1).

In order to rationalize this result, we had to contemplate the intermediacy of an isocyanate derivative, that is, **14** (Scheme 2),<sup>[41]</sup> to account for the "additional" carbonyl residue in the urea **12**.<sup>[42]</sup> Formation of the former could then be explained by reaction of the initial Staudinger reaction intermediate, that is, iminophosphorane **13**, with "CO<sub>2</sub>" in an intermolecular aza-Wittig reaction.<sup>[43]</sup> Finally, addition of the, otherwise-expected reaction product, amine **10**, to isocyanate **14** would lead to the formation of the urea-bridged dimer **12** (Scheme 2).<sup>[44]</sup>



**Scheme 1.** Staudinger reaction of BODIPY-azide **10** leading to urea-bridged bis-BODIPY **12**, rather than to BODIPY-amine, **11**.



**Scheme 2.** Proposed reaction pathway leading to the formation of urea **12**, from BODIPY-azide **11**.

Encouraged by this result, we decided to explore the generality of this process in the formation of urea-bridged bis-BODIPYs by tandem Staudinger/aza-Wittig and amine-isocyanate addition reactions. Thus, hypothesizing that the origin of the required carbon dioxide in the observed transformation could have been absorbed  $\text{CO}_2$  in the employed  $\text{NaOH}$  aqueous solution,<sup>[45]</sup> we decided to evaluate alternative, more reliable,  $\text{CO}_2$  sources.

Accordingly, we first examined the conversion of azide **10** into urea **12** by treatment with  $\text{PPh}_3$  in freshly prepared 1 M aqueous sodium bicarbonate solution.<sup>[46]</sup> However, complete recovery of the starting material was observed after 24 hours. Some conversion could, however, be observed when dry ice was added to a dioxane solution containing azide **10** and  $\text{PPh}_3$ , and the resulting mixture was allowed to stir at room temperature, in a tightly closed vessel, for 48 h. Under these conditions, urea-bridged bis-BODIPY **12** could then be isolated in 10% yield. Finally, a marked improvement in the formation of **12** (98% yield) was observed when a 1,4-dioxane solution of azide **10** and triphenylphosphine, was treated with aqueous triethylammonium hydrogen carbonate buffer (TEAB), as recommended by Azhayev and co-workers.<sup>[47]</sup>

Next, these reaction conditions were applied to various azido-methyl-BODIPYs **8b**, **15a-c**, as summarized in Table 1. All reactions produced the expected dimers in excellent yields, and no apparent effect from the substituents in the pyrrole

**Table 1.** Synthesis of urea-bridged bis-BODIPYs from azido-methyl BODIPYs.

Entry <sup>[a]</sup>	Azide	$\text{R}^1$	$\text{R}^2$	$\text{R}^3$	$\text{R}^4$	Dimer	Yield [%] <sup>[b]</sup>
1	<b>10</b>	Me	Et	Et	Br	<b>12</b>	98
2	<b>8b</b>	H	H	H	H	<b>9</b>	92
3	<b>15a</b>	Me	H	H	H	<b>16a</b>	95
4	<b>15b</b>	Me	Et	Et	H	<b>16b</b>	90
5	<b>15c</b>	Me	H	CHO	H	<b>16c</b>	92

[a] All reactions were carried out with 0.4 mmol of the corresponding azide, at room temperature in dioxane in the presence of  $\text{PPh}_3$  and TEAB buffer. [b] Isolated yields.

moiety could be observed. Thus, the formyl-containing azide **15c**, proved to be a good substrate providing the corresponding urea **16c** in 92% yield. The BODIPY dimers **9**, **16a,b** were purified by column chromatography and fully characterized by  $^1\text{H}$ ,  $^{13}\text{C}$  NMR, and HRMS techniques. These urea-bridged bis-BODIPYs proved to be, chemically stable compounds, readily soluble in common organic solvents such as chloroform, dichloromethane, toluene, acetonitrile, tetrahydrofuran, and methanol.

At this point, it is worth mentioning that under these reaction conditions we have been unable to detect the presence of any amino-methyl BODIPY derivative, for example **11**, (Schemes 1, 2). According to that, it could be assumed that any amino-methyl BODIPY generated in the reaction media was being rapidly consumed by reaction with the postulated BODIPY-isocyanate intermediate, for example, **14** (Scheme 2), to give the urea-bridged adduct, for example, **12** (Scheme 2), which was always obtained in high yields (Table 1).

Along these lines, we hypothesized that addition of an “external” amine to the reaction media could result in the efficient trapping of the intermediate BODIPY-isocyanate to generate non-symmetrical ureas. To test this hypothesis, we performed the reaction of BODIPY-azide **8b** with diethylamine (2.6 equiv) in the presence of  $\text{PPh}_3$  (1.3 equiv) and TEAB buffer (2.6 equiv) in 1,4-dioxane (5 h, room temperature). Under these reaction conditions, urea **17a** was obtained in 93% yield (Figure 3). We could also observe that a drastic reduction in the amount of diethylamine (1.1 equiv rather than 2.6 equiv) resulted in a slightly reduced yield of urea **17a** (83% yield). In order to evaluate the scope of this transformation, which could prove useful in the labeling of amine-containing compounds, we tested the reaction of BODIPY-azides **8b** and **15a** with different primary and secondary amines, and ammonia.

Our results, displayed in Figure 3, show that azido-methyl BODIPYs could be successfully employed for BODIPY conjugation to amino-containing compounds.<sup>[48]</sup> The reaction proceeded well with all amines tested, and good yields of the expected ureas were always obtained.

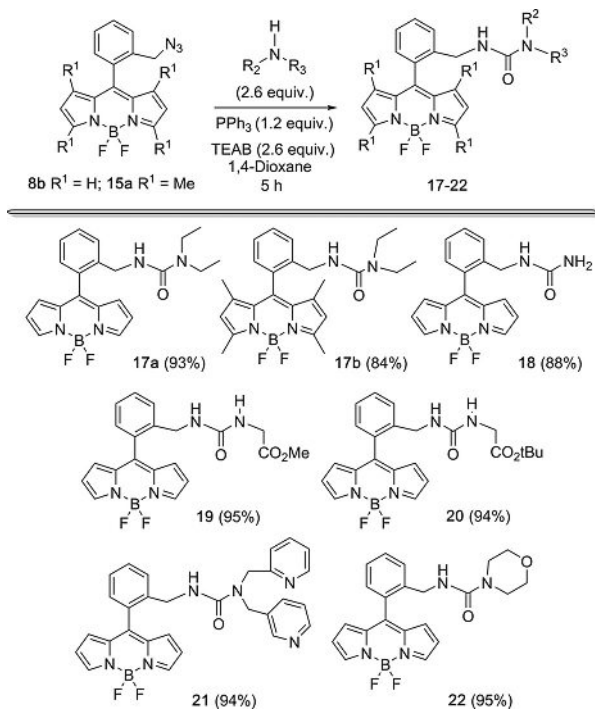


Figure 3. Reaction of azido-methyl BODIPYs **8b** and **15a**, with amines leading to non-symmetrical ureas **17–22**.

### Photophysical properties

The photophysical properties of the new urea-bridged symmetric bis-BODIPYs (whose structure are shown in Table 1) were systematically analyzed in dilute solutions ( $2 \times 10^{-6}$  M) in polar (acetonitrile and ethanol) and apolar (cyclohexane) solvents (Table 2 and Table S1). The absorption profile of these dyads is placed at wavelengths similar to those of the corresponding single counterpart precursors (widely-known by the trademark BDP, for the unsubstituted dipyrrole, PM546, for the

tetramethylated BODIPY, and PM567, for additionally diethylated<sup>[49]</sup> while the absorption probability increases significantly (up to  $16 \times 10^4 \text{ M}^{-1} \text{ cm}^{-1}$ ), becoming roughly twice of each single chromophore (Figure 4). Indeed, the theoretical

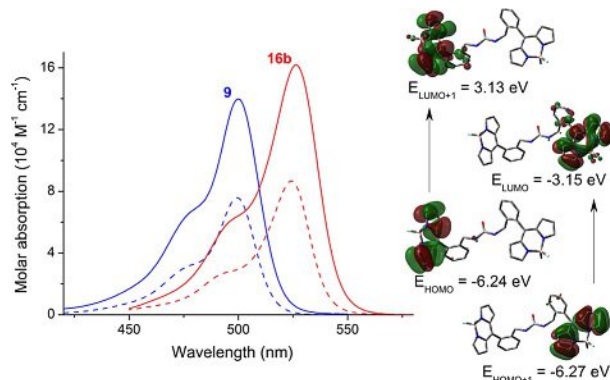


Figure 4. Absorption spectra of the bis-BODIPYs (solid line) derived from BDP (**9**) and PM567 (**16b**), together with the corresponding spectra of the own fragments (dashed). The molecular orbitals involved in the corresponding spectral transitions for **9** are also enclosed.

simulation reveals that the absorption transition results from the contribution of two configurations energetically close (just 0.03 eV), with the electronic density allocated on each dipyrromethane unit. Moreover, after its molecular assembly, both BODIPYs are held apart (distance between center-of-masses longer than 10 Å), hampering any intramolecular interaction between them (see Figure S1). In this configuration, each BODIPY moiety is electronically decoupled retaining its identity and photophysical properties and contributing additionally to the global transition. Furthermore, the 8-aryl unit grafted to each BODIPY is electronically decoupled of the indole core, owing to the steric hindrance exerted by the *ortho*-substitution, and the urea linker is separated from this 8-aryl group by a methylene unit, avoiding, in this way, any resonant interaction among the building blocks of these bridged bis-BODIPYs.

Regarding the emission, and owing to the claimed electronic isolation of the chromophoric units in the dyads, the highly fluorescence efficiency distinctive of BODIPY dyes is retained by these bis-BODIPYs built from BDP, PM546 and PM567 scaffolds in apolar media (cyclohexane, Table 2). Unlike the parent dyes, whose fluorescence was nearly solvent-independent,<sup>[49]</sup> the emission efficiency from the new dyads depends markedly on the polarity of the media. In fact, an increase of the solvent polarity leads to a progressive decrease of the fluorescence efficiency of the new bis-BODIPYs (Figure 5). Moreover, such quenching correlates with a drastic change in the fluorescence decay curves since the time-resolved emission profile acquires a bi-exponential character with the contribution of the shorter-lived component increasing with the solvent polarity (Figure 6).

Table 2. Photophysical (diluted solutions,  $2 \times 10^{-6}$  M of cyclohexane) and lasing (concentrated solutions of ethyl acetate owing to the solubility reasons) properties of the bridged bis-BODIPYs. The corresponding data of the chromophoric units (in grey) are also included for comparison. Photophysical data in solvents of different polarity are listed in Table S1.

Dye	$\lambda_{\text{ab}}$ [nm] <sup>[a]</sup>	$\varepsilon_{\text{max}} \times 10^{-4}$ [M <sup>-1</sup> cm <sup>-1</sup> ] <sup>[b]</sup>	$\lambda_{\text{fl}}$ [nm] <sup>[c]</sup>	$\Delta\nu_{\text{St}}$ [cm <sup>-1</sup> ] <sup>[d]</sup>	$\phi_{\text{f}}^{[e]}$	$\tau$ [ns] <sup>[f]</sup>	C [mM] <sup>[g]</sup>	$\lambda_{\text{la}}$ [nm] <sup>[h]</sup>	% Eff <sup>[i]</sup>
BDP	503.5	7.6	510.5	270	0.96	6.47	1	532	42
<b>9</b>	504.5	14.0	519.0	555	0.83	5.57	0.3	535	46
PM546	499.5	9.7	512.0	490	0.91	5.23	2.5	541	23
<b>16a</b>	502.5	13.4	515.0	485	0.83	5.66	0.9	547	38
PM567	522.5	8.7	539.0	585	0.88	5.60	1.5	566	42
<b>12</b>	528.0	15.5	542.0	490	0.91	6.79	0.5	567	44
<b>16b</b>	525.5	16.2	540.5	530	0.98	6.76	0.4	568	49
<b>16c</b>	499.5	14.0	512.0	490	0.60	0.81(17) 4.50(83)	0.5	559	30

[a] Absorption wavelength. [b] Fluorescence wavelength. [c] Molar absorption coefficient at maximum. [d] Stokes shift. [e] Fluorescence quantum yield. [f] Fluorescence lifetime (for biexponential decays the contribution of each lifetime (%) in indicated between brackets). [g] Optimal concentration for laser measurements. [h] Lasing wavelength. [i] Lasing efficiency.

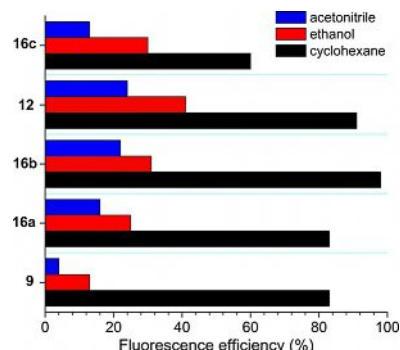


Figure 5. Evolution of the fluorescence quantum yield with the solvent polarity for each urea-bridged symmetric bis-BODIPYs (full data in Table S1).

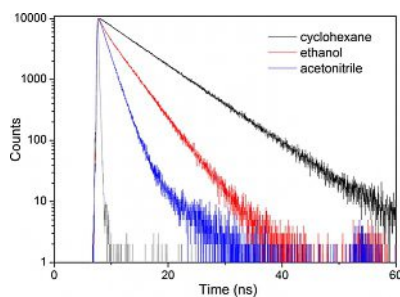


Figure 6. Fluorescence decay curves of representative bis-BODIPY **16b** in solvents of different polarity. Full data in Table S1.

Such marked dependency of the fluorescence signatures on the solvent polarity is often indicative of a quenching process induced by a non-emissive intramolecular charge transfer (ICT) state. In this regard, closely spaced *meso*-linked BODIPY dyads undergoing symmetry-breaking ICT processes have been reported.<sup>[15]</sup> However, such mechanism requires a close and mainly mutual orthogonal disposition of the chromophoric units that is not the structural arrangement of our bridged bis-BODIPYs (see for instance **9** in Figure 4 and Figure S1). Alternatively, in related amide-bridged bis-BODIPYs through the *para*-position of the *meso*-phenyl group, an ICT process between the dye units, whose probability depends on solvent-induced conformational changes, was claimed to explain the recorded fluorescence quenching in polar media.<sup>[29]</sup> The fluorescence of the herein synthesized urea-bridged bis-BODIPYs follows a similar dependence on solvent polarity, supporting that an ICT process is underway. However, the process has to be triggered through a dissimilar mechanism taking into account key structural differences with respect to the above-mentioned amide-bridged bis-BODIPYs such as: 1) the substitution at the, more constrained, *ortho*-position rather than at the *para*-position of the *meso*-phenyl group leads to a more rigid structure; 2) the urea linker reduces the conformational freedom compared to that induced by the more flexible phenanthroline linker bearing side amides, and 3) the already mentioned electronic decoupling of the BODIPY units. These structural features should hamper a closely spaced disposition and hence the probability of an ICT between the electronic clouds of the dyrrin moieties in the present bis-BODIPYs. Moreover, such geo-

metrical arrangement rules out also the probability of excimer formation, which is verified by the absence of long-wavelength shifted fluorescent bands. In fact, we consider that the ICT mechanism consistent with the experimental findings might be a “through space” ICT process from the urea spacer acting as donor, since the electron donor ability of the oxygen is amplified by the flanking amines, to the electron BODIPY core behaving as electron acceptor. Indeed a closer inspection of the optimized geometries (see representative compound **16a** in Figure 7) reveals that the oxygen of the urea spacer tends to

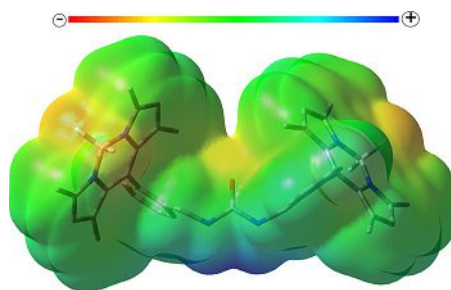


Figure 7. Simulated electrostatic potential mapped onto the electronic density for the bis-BODIPY **16a** in ground state. The corresponding maps for the rest of dyads are enclosed in Figure S1.

be close to the dipyrin planes. Moreover, the corresponding electrostatic maps locate negative charge (in yellow) at the oxygen of the urea bridge, being able to effectively promote ICT processes. As a matter of fact, we have registered the photophysics of the non-dimeric representative compounds **17a** and **17b**, bearing also the mentioned urea group, and that differ exclusively in the substitution pattern of the key BODIPY moiety (Table S2). Whereas the fluorescence quantum yield and lifetime of the methylated compound **17b** remained high and almost the same regardless on the solvent polarity, in dye **17a**, bearing an unsubstituted core, both fluorescence parameters clearly drop in polar media (from 0.83 and 5.75 ns, respectively in cyclohexane to 0.26 and 2.68 ns in acetonitrile). These results support not only the ability of the urea to induce ICT processes, mainly in combination with electron withdrawing BODIPYs, but also suggest that the ICT probability is higher in the dyads than in the single dye. This is reasonable since the dyads bear two electron acceptors (the BODIPY themselves) close to the electron donor urea making the ICT more feasible, and consequently enhancing their fluorescence quenching effectiveness in polar media.

To confirm our hypothesis on the ongoing ICT mechanism, we carefully analyzed the solvent-induced dependence of the fluorescence on the electron donor/acceptor character of the BODIPY core (Figure 5). To this aim, different bis-BODIPYs were rationally designed to modulate their donor/acceptor ability by varying the functionalization (alkyl or formyl) of the dyrrin backbone. The methylation of the chromophoric core softens the solvent-sensitive fluorescence emission. As a matter of fact, the fluorescence efficiency of the bis-BODIPY based on an unsubstituted BDP core (**9**) decreases from 83% in cyclohexane

to merely 4% in more polar media such as acetonitrile, while the tetramethyl substitution at 1-, 3-, 5-, and 7-positions of the dipyrin units (**16a**) allows recording higher fluorescence efficiency in polar media, that is 16% in the same solvent. Subsequent alkylation of the BODIPY core, grafting ethyl moieties at position 2 and 6 of each dipyrin unit (**16b**), promotes a further enhancement of the fluorescence efficiency (22% in acetonitrile) even after *para*-bromination (**12**) of the corresponding 8-phenyl substituents (i.e. 24% in acetonitrile). This behavior is attributed to the inductive electron donor effect exerted by the alkyl moieties grafted to the BODIPY that decreases the electron-withdrawing ability of the chromophoric core and, consequently, hampers the ICT probability from the urea spacer. On the other hand, the C-2 formylation of the tetramethylated dipyrin core (**16c**) induces the opposite effect since the BODIPY core becomes better electron-acceptor enhancing the ICT probability and reducing the fluorescence efficiency (from a 22% on the non-formylated counterpart **16a** to a 13% on formyl derivative **16c**, in acetonitrile as solvent).

To get more insight on the solvent-sensitive fluorescence of these dyads we have also analyzed the photophysical signatures of representative symmetric bis-BODIPYs (**9**, **16a,b**, Table S1) in an electron-donating solvent such as dimethylformamide (DMF). The behavior of the bis-BODIPYs in DMF becomes rather intriguing and striking, showing a marked dependency on the dipyrin alkylation pattern (Figure 8). Due to the high polarity of DMF (described by the Catalan polarity solvent scale,  $S_dP = 0.977$ , as similar to that of acetonitrile, 0.974),<sup>[50]</sup> low fluorescence efficiency and a bi-exponential decay curve, dominated by a short lifetime component, should be expected as result of a further stabilization of the ICT process. However, this behavior was only followed by dyad **9**, derived from the unsubstituted BDP, since when dissolved in DMF exhibits a fluorescence efficiency lower than 5% and a lifetime with a main component (85%) as short as 100 ps (Figure 8 and Table S1). In this case the low chemical stability of the unsubstituted BDP should account, at least to some extent, for this behavior since the solution of this single dye is completely bleached upon addition of DMF (the sample becomes quickly uncolored). Thus, the corresponding dyad **9**, albeit more stable (the loss of color is less marked and slower), likely undergoes such bleaching process that also contributes

to the fluorescence quenching. On the other hand, the dyads derived from more chemically stable dyes, such as PM546 (**16a**) and PM567 (**16b**) display an unexpected behavior. In spite of the high polarity of DMF, which should further stabilize the ICT state, their fluorescence efficiencies increase significantly, raising up to values 37 and 66%, respectively, even higher than those, respectively recorded in less polar solvents like ethanol (Table S1). Regarding the fluorescence decay curves, they tend to recover the typical features of BODIPY dyes (mono-exponential character with lifetimes of 2.71 and 4.08 ns, respectively, Figure 8 and Table S1). Similar fluorescence enhancement was reported by Harriman et al. analyzing dyads based on BODIPYs bearing amide-phenanthroline spacers.<sup>[29]</sup> The unusual behavior induced by DMF should be related not only to its polarity but also to its electron-donor ability (basicity scale,  $SB = 0.613$ ),<sup>[50]</sup> the highest one among the herein selected solvents. The basicity of DMF could induce specific interactions between this hydrogen-bond-acceptor solvent and the proton of the urea linker so long as the electron lone pair of the latter is mainly located on the amine moiety and less shifted to the oxygen atom. In agreement, the positive charge (see the blue color in Figure 7) is located mainly around the nitrogen atoms of the urea, highlighting this position as the most suitable for interaction with electron donor solvents. These interactions have to decrease the electron donor capacity of the urea and, hence, hamper efficiently the probability of the ICT process. Therefore, the fluorescence recorded in DMF arises from the balance between two opposite effects; the high basicity of DMF counterbalances the intrinsic polarity-induced stabilization of the charge separation, hindering the ICT population and yielding higher fluorescence efficiencies and larger lifetimes (mainly in the fully alkylated dyads **16a,b**) than the expected ones according to the solvent polarity.

### Lasing properties

According to the absorption properties of the urea-bridged bis-BODIPYs (Figure 4) their lasing properties were studied under pumping at 355 nm (**9**, **16a** and **16c**) and 532 nm (**12** and **16b**). All the dyes studied in this work exhibit broad-line-width laser emission, with a pump threshold energy of ~0.8 mJ, divergence of 5 mrad and pulse duration of 8 ns full-

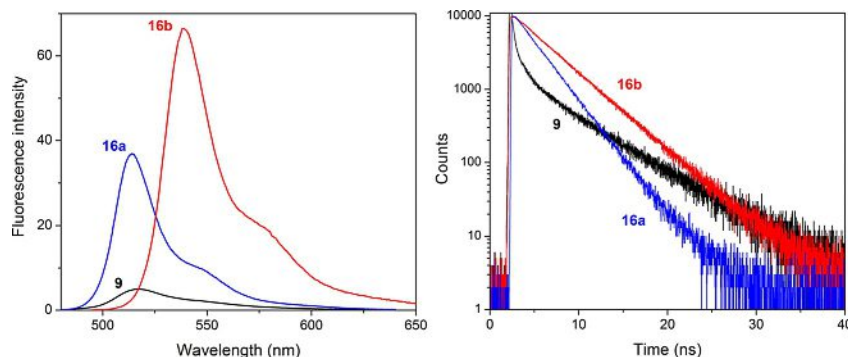


**Figure 8.** Fluorescence spectra (scaled by the fluorescence efficiency) and decay curves of representative symmetric bis-BODIPYs (**9**, **16a,b**) in diluted solutions of DMF.

width at half maximum (FWHM) placed in a simple plane-plane non-tunable resonator cavity. Following the photophysical analysis, the actual effect of the solvent on the dye laser action was analyzed in solutions of polar and apolar solvents. Although the photophysical studies showed that the new derivatives exhibited their highest fluorescence capacity when dissolved in apolar solvents such as cyclohexane (Table 2), the low solubility of BODIPY dyes in this solvent prevents attaining concentrated solutions required for laser experiments. Then, to analyze the dependence of the laser action on the solvent polarity, we carried out the experiments in solvents of increasing polarity enabling, at the same time, good solubility of the new dyes, such as dichloromethane, ethyl acetate, ethanol, and acetonitrile.

To optimize the laser action of the new dyes in the different solvents, firstly, we analysed the dependence of their lasing properties on dye concentration in an ethanolic solution, by varying the optical densities over an order of magnitude while keeping all other experimental parameters constant. The lasing wavelength and efficiency (see Experimental section) of the new dyes at each optimal concentration are presented in Table 2 and Figure 9. Highlight that the optimal concentration

commercial dyes display good photostability under drastic pumping conditions, with the laser emission losing a 50 and a 25% of its efficiency, respectively, after 100 000 pump pulses at 10 Hz repetition rate. The laser action of the new bis-BODIPYs compares well or even enhances that exhibited by their precursors, since their laser efficiencies remain at the initial level without signs of degradation under the same pumping conditions).

The main result that draw our attention is the capacity of the bis-BODIPYs to lase with efficiencies as high as 30% in spite of their fluorescence quantum yields being as low as 0.13 (see **9** in ethanol, Table S1). The rational design linking the BODIPY units in these bis-BODIPYs is key in accounting for its lasing behaviour since it enables at the same time: 1) an absorption increase at the pumping wavelength, which leads to a significantly decrease of the dye concentration in the active medium reducing drastically deleterious effects, such as re-absorption/re-emission and aggregation processes, that becomes particularly important when highly concentrated solutions are required to induce efficient laser emission and 2) a "through-space" ICT process that leads to a very short fluorescence lifetimes, allowing to reach radiative rate constants similar to that observed for other BODIPY dyes. These facts account for the origin and unique features of the laser behaviour of these bis-BODIPYs.

## Conclusion

In summary, we have described a concise and efficient method for the preparation of, chemically stable, urea-bridged bis-BODIPYs from readily available *meso*(*o*-azidomethyl)phenyl BODIPYs. This overall ureation protocol,<sup>[51]</sup> which takes place as a one-pot reaction, involves at least, three processes, namely: i) Staudinger azide→amine transformation, ii) Staudinger azo-Wittig reaction (azide→isocyanate), and iii) the reaction between the so-formed BODIPY-amine and BODIPY-isocyanate to generate the final urea-bridged dimer. Each one of these three steps must occur in a very efficient manner, since isolated yields of the BODIPY dimers normally exceed 90%.

This procedure, which takes place by dimerization of a single BODIPY precursor, contrasts with alternative methods to generate bridged bis-BODIPYs where either a bifunctional spacer is made to react with two BODIPY units,<sup>[11,25]</sup> or where the BODIPY units are constructed around a bifunctionalized (aldehyde, or acid chloride) connector.<sup>[52]</sup> Additionally, we have also shown that *meso*-(*o*-azidomethyl)phenyl BODIPYs are good substrates for the conjugation of BODIPY labels to amine-containing compounds.

The herein-reported urea-bridged symmetric dyads stand out, with both strong absorption in the green-yellow region of the visible spectral region, and a bright fluorescence response in apolar media. Nevertheless, the promotion of an intra-ICT state from the urea-type spacer, acting as a donor, to the dipyrromethane unit, acting as an acceptor, triggers a solvent-sensitive fluorescence in polar media. The probability and extent of this fluorescence quenching can be finely modulated through simple structural modifications to the dipyrromethane

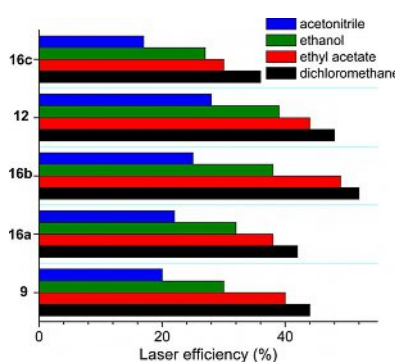


Figure 9. Evolution of the lasing efficiency with the solvent for the symmetric urea-bridged bis-BODIPYs.

for these bis-BODIPYs is about 3-fold lower than those required to induce effective laser action in similar commercial BODIPYs as well as in their mono-BODIPY precursors (Table 2). The lasing behaviour of the new compounds agree with their photophysical properties following the fluorescence quantum yield and the lasing efficiency a similar dependence on both the solvent polarity and the substitution pattern of the BODIPY core: the higher the polarity of the solvent, the lower becomes both the fluorescence quantum yield and the lasing efficiency; the higher is the substitution degree of the BODIPY core, the higher becomes the emission efficiency. In fact, the highest lasing efficiencies are recorded from the PM567 derivatives (**12** and **16b**) in low polar solvents such as dichloromethane where they reach values close to 50% (Figure 9). Photostability is an important feature that defines fluorescent dyes and, in this context, we have analyzed the lasing photostability of PM546 and PM567 as representative for the new bis-BODIPY derivatives (See Experimental section for details). Both single

bone. Thus, alkylated BODIPY scaffolds are desirable to ameliorate the fluorescence efficiency enabling the development of active media for tunable dye lasers with improved absorption of the pumping radiation. In contrast, grafting electron withdrawing moieties at the dipyrin units enhances the probability of the ICT process leading to fluorescent dyes suitable as polarity probes.

In our opinion, this synthetic protocol is not limited to the preparation of symmetric bis-BODIPYs, and its usefulness as a method for the preparation multichromophoric assemblies is under consideration.

## Experimental Section

### General procedure for synthesis of BODIPY dimers from 8-(2-Azidomethylphenyl)-BODIPYs

The appropriate azidomethyl-BODIPY (1 mmol) was added to a mixture of 1 M triethylammonium hydrogen carbonate buffer (2.6 mL) and 1,4-dioxane (6 mL), at room temperature. Triphenylphosphine (1.3 equiv) was added, and the reaction was monitored by TLC. After disappearance of the starting material, the solvent was evaporated in *vacuo* to dryness. The obtained BODIPY dimers were purified by flash chromatography on silica gel.

### General procedure for the reaction of azido-methyl BODIPYs with amines

The appropriate azidomethyl-BODIPY (1 mmol) and the desired amine (2.6 mmol) were added to a mixture of 1 M triethylammonium hydrogen carbonate buffer (2.6 mL) and 1,4-dioxane (12 mL). Triphenylphosphine (1.3 equiv) was next added, and the reaction was monitored by TLC. After disappearance of the starting material, the solvent was evaporated in *vacuo* to dryness. The obtained products were purified by flash chromatography on silica gel.

## Photophysical properties

Diluted solutions (around  $2 \times 10^{-6}$  M) were prepared by adding the corresponding solvent (spectroscopic grade) to the residue from the adequate amount of a concentrated stock solution in acetone, after vacuum evaporation of this solvent. UV/Vis absorption and fluorescence spectra were recorded on a Varian model CARY 4E spectrophotometer and a SPEX Fluorolog 3-22 spectrofluorimeter, respectively. Fluorescence quantum yields ( $\phi$ ) were obtained using the commercial dyes as reference in ethanol, which means; PM546 ( $\phi = 0.85$ , upon excitation at 470 nm) and PM567 ( $\phi = 0.84$ , upon excitation at 490 nm). The values were calculated from corrected spectra (detector sensibility to the wavelength) and corrected by the refractive index of the solvent. Radiative decay curves were registered with the time correlated single-photon counting technique (Edinburgh Instruments, model FL920, with picosecond time-resolution). Fluorescence emission was monitored at the maximum emission wavelength with a multichannel plate detector (Hamamatsu C4878 with 20 ps of time resolution), after excitation at 470 nm by means of a pulsed diode laser (PicoQuant, model LDH470 with full width at half maximum of 40 ps). The fluorescence lifetime ( $\tau$ ) was obtained after the deconvolution of the instrumental response signal from the recorded decay curves by means of an iterative method. The goodness of the exponential fit was controlled by statistical parameters (chi-square and the analysis of the residuals).

## Quantum mechanical calculations

Ground-state geometries were optimized at the density functional theory (DFT) level using the B3LYP hybrid method and the double valence basis set adding polarization functions (6-31g\*). The energy minimization was conducted without any geometrical restriction and the geometries were considered as energy minimum when the corresponding frequency analysis did not give any negative value. The simulation of the absorption spectra (from the ground state geometry) was performed by the time-dependent method (TD-DFT). The solvent effect (ethanol) was also simulated during the calculations by the self consistent reaction field (SCRF) using the polarizable continuum model (PCM). All the theoretical calculations were carried out using the Gaussian 09 implemented in the computational cluster provided by the SGIker resources of the UPV/EHU.

## Lasing properties

Solutions of dyes were contained in 1 cm optical-path rectangular quartz cells carefully sealed to avoid solvent evaporation during the experiments. The liquid solutions were transversely pumped either at 355 nm, with 5 mJ, 8 ns FWHM pulses from the third-harmonic of a Q-switched Nd:YAG laser (Spectron SL282G) or at 532 nm, with 5 mJ, 6 ns FWHM pulses from a frequency-doubled Q-switched Nd:YAG laser (Monocrom OPL-10), at a repetition rate of up to 10 Hz. The exciting pulses were line-focused onto the cell, providing pump fluences on the active medium in the range 110–180 mJ cm<sup>-2</sup>. The oscillation cavity (2 cm length) consisted of a 90% reflectivity aluminum mirror, with the lateral face of the cell as output coupler. The photostability of the dyes was evaluated by irradiating under lasing conditions 10  $\mu$ L of a solution in ethyl acetate. The solutions were contained in a cylindrical Pyrex tube (1 cm height, 1 mm internal diameter) carefully sealed to avoid solvent evaporation during the experiments. Although the low optical quality of the capillary tube prevents laser emission from the dyes, information about photostabilities can be obtained by monitoring the decrease in laser-induced fluorescence intensity, excited transversally to the capillary tube, as a function of the number of pump pulses at 10 Hz repetition rate. The fluorescence emission was monitored perpendicular to the exciting beam, collected by an optical fiber, and imaged onto the input slit of a monochromator (Acton Research corporation) and detected with a charge-coupled device (CCD) (SpectruMM:GS128B). The fluorescence emission was recorded by feeding the signal to the boxcar (Stanford Research, model 250) to be integrated before being digitized and processed by a computer. Each experience was repeated at least three times. The estimated error in the energy and photostability measurements was 10%.

## Acknowledgements

Financial support from *Ministerio de Economía y Competitividad* (MINECO, Spain) grants CTQ2015-66702-R, MAT2015-68837-REDT, and MAT2014-51937-C3-1-P, MAT2014-51937-C3-1-P and -3-P, and *Departamento de Educación, Gobierno Vasco* (IT912-16) is gratefully acknowledged. We thank Ms. Marina Rodríguez-Yáñez for skillful assistance.

## Conflict of interest

The authors declare no conflict of interest.

**Keywords:** aza-Wittig • charge transfer • fluorescence • Staudinger reaction • ureation

[1] A. Treibs, F.-H. Kreuzer, *Liebigs Ann. Chem.* **1968**, *718*, 208–223.

[2] a) A. Loudet, K. Burgess, *Chem. Rev.* **2007**, *107*, 4891–4932; b) G. Ulrich, R. Ziessel, A. Harriman, *Angew. Chem. Int. Ed.* **2008**, *47*, 1184–1201; *Angew. Chem.* **2008**, *120*, 1202–1219; c) R. Ziessel, G. Ulrich, A. Harriman, *New J. Chem.* **2007**, *31*, 496–501.

[3] a) Y. Cakmak, E. U. Akkaya, *Org. Lett.* **2009**, *11*, 85–88; b) V. Lakshmi, R. R. Rao, M. Ravikanth, *Org. Biomol. Chem.* **2015**, *13*, 2501–2517; c) N. Boens, B. Verbelen, W. Dehaen, *Eur. J. Org. Chem.* **2015**, 6577–6595; d) C. F. A. Gómez-Durán, I. Esnal, I. Valois-Escamilla, A. Urias-Benavides, J. Bañuelos, I. Lopez Arbeloa, I. García-Moreno, E. Peña-Cabrera, *Chem. Eur. J.* **2016**, *22*, 1048–1061.

[4] a) J. Bañuelos, *Chem. Rec.* **2016**, *16*, 335–348; b) V. Lakshmi, R. Sharma, M. Ravikanth, *Rep. Org. Chem.* **2016**, *6*, 1–24; c) H. Lu, J. Mack, Y. Yang, Z. Shen, *Chem. Soc. Rev.* **2014**, *43*, 4778–4823.

[5] S. G. Awuah, Y. You, *RSC Adv.* **2012**, *2*, 11169–11183.

[6] a) N. Boens, V. Leen, W. Dehaen, *Chem. Soc. Rev.* **2012**, *41*, 1130–1172; b) T. Kowada, H. Maeda, K. Kikuchi, *Chem. Soc. Rev.* **2015**, *44*, 4953–4972.

[7] D. Zhang, V. Martin, I. García-Moreno, A. Costela, M. E. Perez-Ojeda, Y. Xiao, *Phys. Chem. Chem. Phys.* **2011**, *13*, 13026–13033.

[8] a) R. Ziessel, G. Ulrich, A. Haefele, A. Harriman, *J. Am. Chem. Soc.* **2013**, *135*, 11330–11344; b) M. A. H. Alamiy, A. Harriman, A. Haefele, R. Ziessel, *ChemPhysChem* **2015**, *16*, 1867–1872.

[9] a) A. Kamkaew, S. H. Lim, H. B. Lee, L. V. Kiew, L. Y. Chung, K. Burgess, *Chem. Soc. Rev.* **2013**, *42*, 77; b) J. Fan, M. Hu, P. Zhan, X. Peng, *Chem. Soc. Rev.* **2013**, *42*, 29–43; c) A. Bessette, G. S. Hanan, *Chem. Soc. Rev.* **2014**, *43*, 3342–3405; d) J. Zhao, J. K. Xu, W. Yang, Z. Wang, F. Zhong, *Chem. Soc. Rev.* **2015**, *44*, 8904–8939; e) Y. Ge, D. F. O’Shea, *Chem. Soc. Rev.* **2016**, *45*, 3846–3864. For recent applications, see: f) N. Maindron, M. Ipuv, C. Bernhard, D. Lhenry, M. Moreau, S. Carme, A. Oudot, B. Collin, J.-M. Vrigneaud, P. Provent, F. Brunotte, F. Denat, C. Goze, *Chem. Eur. J.* **2016**, *22*, 12670–12674; g) D. Lhenry, M. Larrouy, C. Bernhard, V. Goncalves, O. Raguin, P. Provent, M. Moreau, B. Collin, A. Oudot, J.-M. Vrigneaud, F. Brunotte, C. Goze, F. Denat, *Chem. Eur. J.* **2015**, *21*, 13091–13099; h) L. G. Meimetis, E. Boros, J. C. Carlson, C. Ran, P. Caravan, R. Weissleder, *Bioconjugate Chem.* **2016**, *27*, 257–263; i) S. Liu, D. Li, Z. Zhang, G. K. S. Prakash, P. S. Conti, Z. Li, *Chem. Commun.* **2014**, *50*, 7371–7373; j) S. Liu, T.-P. Lin, D. Li, L. Leamer, H. Shan, Z. Li, F. P. Gabai, P. S. Conti, *Theranostics* **2013**, *3*, 181–189.

[10] J. Ahrens, B. Böker, K. Brandhorst, M. Funk, M. Bröring, *Chem. Eur. J.* **2013**, *19*, 11382–11395.

[11] S. Zrig, P. Remy, B. Andrioletti, E. Rose, I. Asselberghs, K. Clays, *J. Org. Chem.* **2008**, *73*, 1563–1566.

[12] a) M. Bröring, F. Bregier, R. Kruger, C. Kleeberg, *Eur. J. Inorg. Chem.* **2008**, 5505–5512; b) M. Bröring, R. Kruger, S. Link, C. Kleeberg, S. Kohler, X. Xie, B. Ventura, L. Flamigni, *Chem. Eur. J.* **2008**, *14*, 2976–2983; c) B. Ventura, G. Marconi, M. Bröring, R. Kruger, L. Flamigni, *New J. Chem.* **2009**, *33*, 428–438; a. B. Nepomnyashchii, M. Bröring, J. Ahrens, A. J. Bard, *J. Am. Chem. Soc.* **2011**, *133*, 19498–19504.

[13] a) S. Rihm, M. Erdem, A. De Nicola, P. Retailleau, R. Ziessel, *Org. Lett.* **2011**, *13*, 1916–1919; b) Y. Hayashi, S. Yamaguchi, W. Y. Cha, D. Kim, H. Shinokubo, *Org. Lett.* **2011**, *13*, 2992–2995; c) A. B. Nepomnyashchii, M. Bröring, J. Ahrens, A. J. Bard, *J. Am. Chem. Soc.* **2011**, *133*, 8633–8645; d) L. Gai, H. Lu, B. Zou, G. Lai, Z. Shen, Z. Li, *RSC Adv.* **2012**, *2*, 8840–8846; e) Z. Li, Y. Chen, X. Lv, W.-F. Fu, *New J. Chem.* **2013**, *37*, 3755–3761.

[14] a) Y. Cakmak, S. Kolemen, S. Duman, Y. Dede, Y. Dolen, B. Kilic, Z. Kostereli, L. T. Yildirim, A. L. Dogan, D. Guc, E. U. Akkaya, *Angew. Chem. Int. Ed.* **2011**, *50*, 11937–11941; *Angew. Chem.* **2011**, *123*, 12143–12147; b) W. Pang, X.-F. Zhang, J. Zhou, C. Yu, E. Hao, L. Jiao, *Chem. Commun.* **2012**, 48, 5437–5439; c) S. Kolemen, Y. Cakmak, Z. Kostereli, E. U. Akkaya, *Org. Lett.* **2014**, *16*, 660–663.

[15] M. T. Whited, N. M. Patel, S. T. Roberts, K. Allen, P. I. Djurovich, S. E. Bradforth, M. E. Thompson, *Chem. Commun.* **2012**, *48*, 284–286.

[16] A. B. Nepomnyashchii, A. J. Bard, *Acc. Chem. Res.* **2012**, *45*, 1844–1853.

[17] a) S. Abbate, T. Bruhn, G. Pesticelli, G. Longhi, *J. Phys. Chem. A* **2017**, *121*, 394–400; b) S. Stachelek, A. Harriman, *J. Phys. Chem. A* **2016**, *120*, 8104–8113; c) S. Knippenberg, M. W. Bohnwagner, P. H. P. Harbach, A. Dreuw, *J. Phys. Chem. A* **2015**, *119*, 1323–1331; d) T. Bruhn, G. Pesticelli, S. Jurinovich, A. Schaunlöffel, F. Witterauf, J. Ahrens, M. Bröring, G. Bringmann, *Angew. Chem. Int. Ed.* **2014**, *53*, 14592–14595; *Angew. Chem.* **2014**, *126*, 14821–14824; e) S. Duman, Y. Cakmak, S. Kolemen, E. U. Akkaya, Y. Dede, *J. Org. Chem.* **2012**, *77*, 4516–4527.

[18] W. Wu, X. Cui, J. Zhao, *Chem. Commun.* **2013**, *49*, 9009–9011.

[19] a) L. Yuan, W. Lin, K. Zheng, L. He, W. Huang, *Chem. Soc. Rev.* **2013**, *42*, 622–661; b) V. V. Roznyatovskiy, C.-H. Leeb, J. L. Sessler, *Chem. Soc. Rev.* **2013**, *42*, 1921–1933.

[20] a) M. Nakamura, H. Tahara, K. Takahashi, T. Nagata, H. Uoyama, D. Kuzuhara, S. Mori, T. Okujima, H. Yamada, H. Uno, *Org. Biomol. Chem.* **2012**, *10*, 6840–6849; b) A. Wakamiya, T. Murakami, S. Yamaguchi, *Chem. Sci.* **2013**, *4*, 1002–1007; c) H. Yokoi, N. Wachi, S. Hiroto, H. Shinokubo, *Chem. Commun.* **2014**, *50*, 2715–2717; d) M. Nakamura, M. Kitatsuka, K. Takahashi, T. Nagata, S. Mori, D. Kuzuhara, T. Okujima, H. Yamada, T. Nakaea, H. Uno, *Org. Biomol. Chem.* **2014**, *12*, 1309–1317; e) C. Yu, L. Jiao, T. Li, Q. Wu, W. Miao, J. Wang, Y. Wei, X. Mu, E. Hao, *Chem. Commun.* **2015**, *51*, 16852–16855; f) J. Wang, Q. Wu, S. Wang, C. Yu, J. Li, E. Hao, Y. Wei, X. Mu, L. Jiao, *Org. Lett.* **2015**, *17*, 5360–5363; g) Y. Ni, S. Lee, M. Son, N. Aratani, M. Ishida, A. Samanta, H. Yamada, Y.-T. Chang, H. Furuta, D. Kim, J. Wu, *Angew. Chem. Int. Ed.* **2016**, *55*, 2815–2819; *Angew. Chem.* **2016**, *128*, 2865–2869.

[21] P. E. Kesavan, S. Das, M. Y. Lone, P. C. Jha, S. Moric, I. Gupta, *Dalton Trans.* **2015**, *44*, 17209–17221.

[22] a) F. Bergström, I. Mikhalyov, P. Hägglof, R. Wortmann, T. Ny, L. B.-Å. Johansson, *J. Am. Chem. Soc.* **2002**, *124*, 196–204; b) I. Mikhalyov, N. Gretskaya, F. Bergström, L. B.-Å. Johansson, *Phys. Chem. Chem. Phys.* **2002**, *4*, 5663–5670; c) A. Poirel, A. De Nicola, P. Retailleau, R. Ziessel, *J. Org. Chem.* **2012**, *77*, 7512–7525; d) N. Sakamoto, C. Ikeda, M. Yamamura, T. Nabeshima, *Chem. Commun.* **2012**, *48*, 4818–4820; e) E. M. Sánchez-Carnerero, F. Moreno, B. L. Maroto, A. R. Agarrabeitia, J. Bañuelos, T. Arbeloa, I. Lopez-Arbeloa, M. J. Ortiz, S. de la Moya, *Chem. Commun.* **2013**, *49*, 11641–11643; f) J. Ahrens, A. Scheja, R. Wicht, M. Bröring, *Eur. J. Org. Chem.* **2016**, 2864–2870; g) J. Ahrens, B. Cordes, R. Wicht, B. Wolfram, M. Bröring, *Chem. Eur. J.* **2016**, *22*, 10320–10325; h) C. Ray, E. M. Sanchez-Carnerero, F. Moreno, B. L. Maroto, A. R. Agarrabeitia, M. J. Ortiz, I. Lopez-Arbeloa, J. Bañuelos, K. D. Cohovi, J. L. Lunkley, G. Muller, S. de la Moya, *Chem. Eur. J.* **2016**, *22*, 8805–8808; i) C. Ray, J. Bañuelos, T. Arbeloa, B. L. Maroto, F. Moreno, A. R. Agarrabeitia, M. J. Ortiz, I. Lopez-Arbeloa, S. de la Moya, *Dalton Trans.* **2016**, *45*, 11839–11848.

[23] a) J. Ahrens, B. Haberlag, A. Scheja, M. Tamm, M. Bröring, *Chem. Eur. J.* **2014**, *20*, 2901–2912; b) H. Yokoi, S. Hiroto, H. Shinokubo, *Org. Lett.* **2014**, *16*, 3004–3006.

[24] C. Goze, G. Ulrich, R. Ziessel, *Org. Lett.* **2006**, *8*, 4445–4448.

[25] N. Saki, P. T. Dinc, E. U. Akkaya, *Tetrahedron* **2006**, *62*, 2721–2725.

[26] W. Duan, H. Wei, T. Cui, B. Gao, *J. Mater. Chem. B* **2015**, *3*, 894–898.

[27] S. Mula, G. Ulrich, R. Ziessel, *Tetrahedron Lett.* **2009**, *50*, 6383–6388.

[28] a) A. C. Benniston, G. Copley, A. Harriman, D. Howgego, R. W. Harrington, W. Clegg, *J. Org. Chem.* **2010**, *75*, 2018–2027; b) M. A. H. Alamiy, A. C. Benniston, G. Copley, A. Harriman, D. Howgego, *J. Phys. Chem. A* **2011**, *115*, 12111–12119.

[29] S. Thakare, P. Stachelek, S. Mula, A. B. More, S. Chattopadhyay, A. K. Ray, N. Sekar, R. Ziessel, A. Harriman, *Chem. Eur. J.* **2016**, *22*, 14356–14366.

[30] M. R. Martinez-Gonzalez, A. Urias-Benavides, E. Alvarado-Martínez, J. C. Lopez, A. M. Gómez, M. del Rio, I. García, A. Costela, J. Bañuelos, T. Arbeloa, I. Lopez Arbeloa, E. Peña-Cabrera, *Eur. J. Org. Chem.* **2014**, 5659–5663.

[31] L. S. Liebeskind, J. Srögl, *J. Am. Chem. Soc.* **2000**, *122*, 11260–11261.

[32] E. Peña-Cabrera, A. Aguilar-Aguilar, M. Gonzalez-Dominguez, E. Lager, R. Zamudio-Vazquez, J. Godoy-Vargas, F. Villanueva-Garcia, *Org. Lett.* **2007**, *9*, 3985–3988.

[33] R. I. Roacho, A. J. Metta-Magaña, E. Peña-Cabrera, K. H. Pannell, *J. Phys. Org. Chem.* **2013**, *26*, 345–351.

[34] M. del Río, F. Lobo, J. C. Lopez, A. Oliden, J. Bañuelos, I. Lopez-Arbeloa, I. García Moreno, A. M. Gómez, *J. Org. Chem.* **2017**, *82*, 1240–1247.

[35] N. Volz, J. Clayden, *Angew. Chem. Int. Ed.* **2011**, *50*, 12148–12155; *Angew. Chem.* **2011**, *123*, 12354–12361.

[36] a) J. Chen, A. Burghart, A. Derecskei-Kovacs, K. Burgess, *J. Org. Chem.* **2000**, *65*, 2900–2906; b) I. V. Sazanovich, C. Kirmaier, E. Hindin, L. Yu, D. F. Bocian, J. S. Lindsey, D. Holten, *J. Am. Chem. Soc.* **2004**, *126*, 2664–2665.

[37] a) R. Ziessel, L. Bonardi, P. Retailleau, G. Ulrich, *J. Org. Chem.* **2006**, *71*, 3093–3102; b) R. Ziessel, L. Bonardi, G. Ulrich, *Dalton Trans.* **2006**, 2913–2918.

[38] V. Blažek Bregović, N. Basarić, K. Mlinarić-Majerski, *Coord. Chem. Rev.* **2015**, *295*, 80–124.

[39] a) E. Ganapathi, S. Madhu, T. Chatterjee, R. Gonnade, M. Ravikanth, *Dyes Pigm.* **2014**, *102*, 218–227; b) J. Liu, X. He, J. Zhang, T. He, L. Huang, J. Shen, D. Li, H. Qiu, S. Yin, *Sens. Actuators B* **2015**, *208*, 538–545; c) M. Formica, V. Fusi, L. Giorgi, G. Piersanti, M. Retini, *Tetrahedron* **2016**, *72*, 7039–7049.

[40] a) H. Staudinger, J. Meyer, *Helv. Chim. Acta* **1919**, *2*, 635–646; b) Y. G. Gololobov, I. N. Zhmurova, L. F. Kasukhin, *Tetrahedron* **1981**, *37*, 437–472; c) Y. G. Gololobov, L. F. Kasukhin, *Tetrahedron* **1992**, *48*, 1353–1406.

[41] S. Bräse, C. Gil, K. Knepper, V. Zimmermann, *Angew. Chem. Int. Ed.* **2005**, *44*, 5188–5240; *Angew. Chem.* **2005**, *117*, 5320–5374.

[42] D. Carnaroglio, K. Martina, G. Palmisano, A. Penoni, C. Domini, G. Cravotto, *Beilstein J. Org. Chem.* **2013**, *9*, 2378–2386.

[43] P. Friant-Michel, A. Marsurab, J. Kovacs, I. Pinter, J.-L. Rivail, *J. Mol. Struct.* **1997**, *395*–396, 61–69.

[44] J. P. Collman, Z. Wang, A. Straumanis, *J. Org. Chem.* **1998**, *63*, 2424–2425.

[45] For studies regarding absorption of CO<sub>2</sub> into aqueous solutions of alkali hydroxides see: a) J. B. Tepe, B. F. Dodge, *Trans. Am. Inst. Chem. Eng.* **1943**, *39*, 255–276; b) R. Pohorecki, W. Moniuk, *Chem. Eng. Sci.* **1988**, *43*, 1677–1684; c) S. Gondal, N. Asif, H. F. Svendsen, H. Knuutila, *Chem. Eng. Sci.* **2015**, *123*, 487–499.

[46] In the reaction of NaOH with atmospheric CO<sub>2</sub>, the main product is NaHCO<sub>3</sub>: J.-G. Shim, D. W. Lee, J. H. Lee, N.-S. Kwak, *Environ. Eng. Res.* **2016**, *21*, 297–303.

[47] A. Yagodkin, K. Loschcke, J. Weisell, A. Azhayev, *Tetrahedron* **2010**, *66*, 2210–2221.

[48] a) X. Li, X. Gao, W. Shi, H. Ma, *Chem. Rev.* **2014**, *114*, 590–659; b) M. Sintes, F. De Moliner, D. Caballero-Lima, D. W. Denning, N. D. Read, N. Kielland, M. Vendrell, R. Lavilla, *Bioconjugate Chem.* **2016**, *27*, 1430–1434; c) M. Sunbul, L. Nacheva, A. Jäschke, *Bioconjugate Chem.* **2015**, *26*, 1466–1469; d) T. Felbeck, K. Hoffmann, M. M. Lezhnina, U. H. Kynast, U. Resch-Genger, *J. Phys. Chem. C* **2015**, *119*, 12978–12987.

[49] F. López Arbeloa, J. Bañuelos, V. Martínez, T. Arbeloa, I. López Arbeloa, *Int. Rev. Phys. Chem.* **2005**, *24*, 339–374.

[50] J. Catalán, *J. Phys. Chem. B* **2009**, *113*, 5951–5960.

[51] G. Godeau, F. Guittard, T. Darmanin, *Mater. Today Commun.* **2016**, *8*, 165–171.

[52] H. Qi, J. J. Teesdale, R. C. Pupillo, J. Rosenthal, A. J. Bard, *J. Am. Chem. Soc.* **2013**, *135*, 13558–13566.

Manuscript received: July 21, 2017

Accepted manuscript online: August 29, 2017

Version of record online: October 9, 2017